

## HYDROGEN-ASSISTED FRACTURE OF WELDED AISI 316 AUSTENITIC STAINLESS STEEL

*X. Tang and G.H. Schiroky,  
Swagelok Company, Solon, OH, USA*

*C. San Marchi and B.P. Somerday,  
Sandia National Laboratories, Livermore, CA, USA*

### ABSTRACT

AISI 316 austenitic stainless steel is a preferred material of construction for valves, fittings, and other fluid system components for high-pressure gaseous hydrogen service. The interaction of hydrogen with stainless steel depends on the prevailing stress-state and the microstructural characteristics of a component's material of construction, among other variables. To evaluate the effects of geometrical stress-risers and two-phase microstructures on hydrogen-assisted fracture of AISI 316 stainless steel, smooth and notched tensile properties were measured for annealed material as well as for autogenously welded specimens after thermal precharging with hydrogen. The tensile ductility of welded microstructures is significantly reduced by hydrogen precharging, and the addition of a notch further degrades ductility. These observations are rationalized in terms of hydrogen-enhanced localized plasticity.

### INTRODUCTION

Hydrogen gas is increasingly being considered as an energy storage medium for stationary and mobile power generation. Fluid system components for hydrogen delivery, containment and refueling, such as filling nozzles, receptacles, tubing, fittings and valves must retain satisfactory mechanical properties when they are in contact with high pressure hydrogen over an anticipated operating temperature range of -50°C to 100°C.

The mechanical properties of many metallic materials can be affected by hydrogen gas, especially when gas pressure is high. Hydrogen-induced property degradation of materials has been studied for many decades [1-7]. Austenitic stainless steels in general are more resistant to hydrogen-assisted fracture than ferritic steels [7]. Among the austenitic stainless steels, the AISI 316 family of alloys represents particularly attractive candidates for hydrogen system components. Recently published results show that the composition of AISI 316 stainless steel has a rather significant effect on the material's resistance to hydrogen-assisted fracture [8] and that the effect of hydrogen on property degradation becomes even more evident at sub-ambient temperatures [9, 10]. In particular, these studies show that AISI 316 alloys with the minimally required content of 10% nickel are much more affected by hydrogen than the properties of alloys with more than 12% nickel [8-10].

The objective of this study was to evaluate additional effects of hydrogen-induced property degradation that may be observed in components with stress risers such as sharp corners and notches, and with welds. Weld zones tend to have two-phase dendritic microstructures (similar to casting microstructures) because ferrite is desirable during solidification of austenitic stainless steels in fusion welding processes to prevent weld cracking. Consequently, since ferritic stainless steels are typically not as resistant to degradation by hydrogen as austenitic stainless steels [7], ferrite-containing welds in AISI 316 may be more susceptible to hydrogen-assisted fracture. In this study, hydrogen effects on both smooth and notched tensile properties of non-welded and welded specimens were determined and compared.

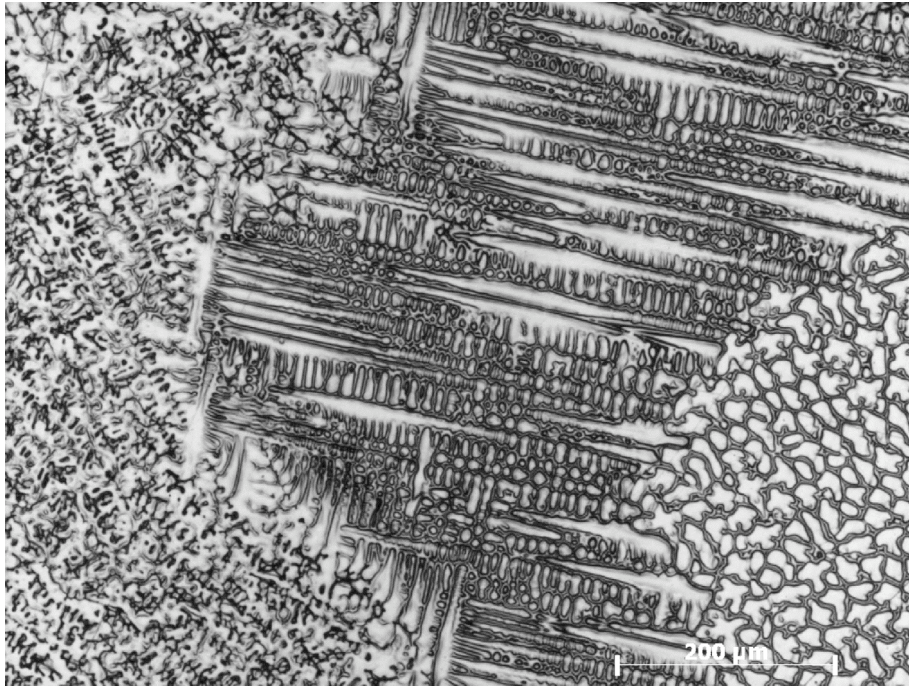


Figure 1: Microstructure of the fusion zone in the welds produced in this study.

## EXPERIMENTAL

The AISI 316L stainless steel used in this study (Table 1) is the same heat of material as alloy E in Refs. [8, 9]. This material was produced by electric arc furnace (EAF) melting, argon oxygen decarburization (AOD) and vacuum arc remelting (VAR). Materials refined by VAR have low levels of residual elements and improved compositional homogeneity. The welded tensile bars were produced by orbital autogenous gas tungsten arc welding of cylindrical butt joints; since filler was

not used, the average chemical compositions of welds and base metal are identical. The welded specimens were produced from material in the strain-hardened condition; however, welding yields nominally annealed microstructures in the heat-affected zone (HAZ) adjacent to the fusion zone. The full-penetration welds were centered in the gauge length of the test specimens. Figure 1 shows an example of the significant microstructural variation found in the fusion zone of the welds.

*Table 1: Alloy composition (weight percent).*

| C     | Cr    | Ni    | Mo   | Mn   | Si   | P     | S     | N    |
|-------|-------|-------|------|------|------|-------|-------|------|
| 0.022 | 17.55 | 13.25 | 2.70 | 1.16 | 0.63 | 0.015 | 0.006 | 0.04 |

Two types of tensile specimens were used in this study: smooth and notched. The ASTM E8 subsized smooth tensile specimens had a gauge diameter of 4 mm. The gauge length consists of the fusion zone, HAZ, and strain-hardened material. The notched tensile specimens were proportionally scaled from the standard specimen that is suggested in ASTM G142. The V-notch has an included angle of 60°, the major and minor diameters are 8 and 4 mm respectively, and the notch root radius is nominally 0.05 mm. For the welded specimens, notches were located either in the fusion zone or in the heat-affected zone (HAZ) approximately 1 mm from the center of the fusion zone; specimens with notches in these two locations are referred to as the weld and HAZ respectively.

All tensile testing was conducted at constant displacement rate: smooth specimens at 0.02 mm/s and notched specimens at 0.002 mm/s. The measured strain rate for the smooth tensile specimens was approximately  $1.5 \times 10^{-3}$  /s (in the plastic regime). Yield strength ( $S_y$ , 0.2% offset), tensile strength ( $S_u$ ), and reduction of area (RA) are reported for the smooth tensile tests. Notched tensile strength ( $\sigma_S$ ) and RA are reported for the notched tensile tests. Reported values are an average of at least two measurements.

Thermal precharging of the final machined specimens was achieved in 138 MPa H<sub>2</sub> gas at 300°C for at least 20 days. This length of time is sufficient to ensure that the hydrogen concentration was essentially uniform across the largest diameter of the specimens based on predictions for hydrogen diffusion. Details of this thermal precharging process can be found elsewhere [6]. The hydrogen concentration in the tested specimens was measured to be approximately 140 ppm by weight, consistent with other work [11].

Fracture surfaces of the tensile tested specimens were examined using scanning electronic microscope (SEM).

## RESULTS AND DISCUSSIONS

### Smooth Tensile Properties

The tensile strength of the welded smooth specimens is approximately the same as the annealed base material. The yield strength, however, is slightly higher for the welded specimens, probably due to constraint provided by the strain-hardened starting material adjacent to the HAZ. In contrast to the strength, the RA of the welded specimens (69%) is clearly lower than the base material (83%). This difference is likely related to the higher defect population intrinsic to weld (cast) microstructures.

Internal hydrogen leads to a significant increase of strength for both the annealed and welded specimens (Table 2), similar to previous reports on austenitic stainless steels [6-9]. Tensile elongation is generally not used to evaluate hydrogen-assisted fracture in austenitic stainless steels and previous work has shown that elongation is relatively insensitive to high concentrations of internal hydrogen [6-9]. Reduction of area (RA), on the other hand, is particularly sensitive to hydrogen and commonly used for evaluation of hydrogen-assisted fracture. As previously reported [8], wrought AISI 316 stainless steels experience moderate reduction of RA when thermally precharged with hydrogen. Welded material, however, experiences significantly greater loss of ductility due to internal hydrogen than the annealed material (Table 2). Austenite-ferrite microstructures tend to be more sensitive to hydrogen-assisted fracture than single-phase austenite [12, 13], which may explain the lower RA for the welded specimens. Similar values of RA have been reported elsewhere for both non-charged and hydrogen-precharged austenitic stainless steel welds [14].

Table 2: Smooth tensile properties of AISI type 316L austenitic stainless steel

| Specimen                 | Condition    | S <sub>y</sub><br>(MPa) | S <sub>u</sub><br>(MPa) | RA<br>(%) |
|--------------------------|--------------|-------------------------|-------------------------|-----------|
| Annealed<br>(Non-welded) | non-charged  | 242                     | 585                     | 83        |
|                          | H-precharged | 301                     | 631                     | 72        |
| Welded                   | non-charged  | 272                     | 572                     | 69        |
|                          | H-precharged | 323                     | 623                     | 43        |

### Notched Tensile Properties

The notched tensile strength of the welded specimens is nominally the same as the annealed base material (Table 3). The notched tensile strength of the HAZ specimens is slightly higher, probably due to incomplete annealing of the strain-hardened microstructure during welding. The ductility (as measured by RA) is significantly lower in the weld and HAZ specimens (22 and 26% respectively) compared to the annealed base material (43%).

Hydrogen precharging increases the notched tensile strength of the annealed base material (Table 3), similar to smooth specimens. The strength of the hydrogen-precharged weld and HAZ appears to decrease slightly compared to the non-charged weld and HAZ respectively; however, these differences are essentially within the variation of these measurements. Hydrogen-precharging reduces RA of the annealed, welded and HAZ specimens to greater extent in notched specimens than in smooth specimens (Table 3). The RA of hydrogen-precharged, notched specimens is greatest for the HAZ (23%) and lowest for the welded specimens (13%).

AISI 316 stainless steel is generally considered to be notch insensitive, since the notched tensile strength ( $\sigma_s$ ) is significantly greater than the unnotched tensile strength. The high RA of the annealed base material (43%) also demonstrates the inherent ductility of this microstructure, which implies notch insensitive behavior. Lower RA for notched specimens compared to smooth specimens (83%) is expected due to the triaxial state of stress generated by the presence of the notch. The notched tensile strength is relatively unaffected by internal hydrogen, while the RA is significantly degraded by internal hydrogen for all the tested conditions. These observations show that while hydrogen affects the deformation in these microstructures, fracture is associated with macroscopic plasticity. This is explored in more detail in the following section.

*Table 3: Notched tensile properties of AISI type 316L austenitic stainless steel.*

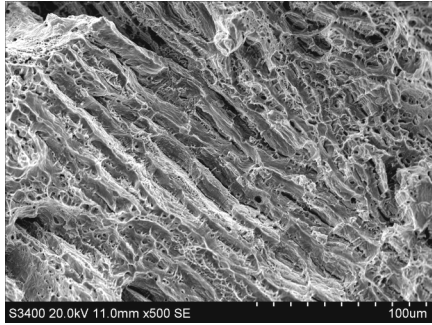
| Specimen                 | Condition    | $\sigma_s$<br>(MPa) | RA<br>(%) |
|--------------------------|--------------|---------------------|-----------|
| Annealed<br>(Non-welded) | non-charged  | 850                 | 43        |
|                          | H-precharged | 904                 | 18        |
| Weld                     | non-charged  | 854                 | 22        |
|                          | H-precharged | 843                 | 13        |
| HAZ                      | non-charged  | 936                 | 26        |
|                          | H-precharged | 926                 | 23        |

### Fracture Mode

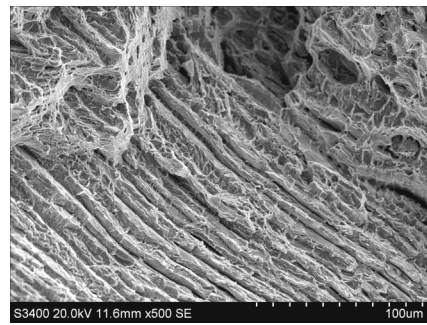
AISI type 316 austenitic stainless steels are very ductile materials that typically display dimpled fracture surfaces that are indicative of microvoid coalescence (MVC). The characteristics of MVC are observed for both the annealed and welded tensile specimens fractured in this study. The welded specimens also display localized areas that appear to reflect the solidified microstructure inherent in fusion welds (Figure 2). Although no evidence of weld cracking was observed, the Cr-Ni ratio (Hammer equivalents) for this material is 1.5, which corresponds to the empirical compositional boundary for susceptibility to weld cracking in austenitic stainless steel [15]. Despite fracture features associated with the welded

microstructure and the potential for weld cracking in these welds, the measured tensile ductility is consistent with quality welds that feature only MVC [14].

The observed fracture modes for the welded specimens are essentially unchanged by hydrogen-precharging. The majority of the fracture surface shows evidence of microvoid coalescence (Figure 3). The underlying solidification microstructure, however, is more apparent on the fracture surfaces of hydrogen-precharged, smooth specimens than the non-charged specimens (Figure 2), covering about one-third of the fracture surface of the hydrogen-precharged specimens. Ductile dimples characterize the fracture appearance near the center of the notched specimens for all the tested materials and conditions. The prevalence of MVC underscores the inherently ductile nature of these materials and microstructures despite high concentrations of hydrogen. The data (Tables 2 and 3), however, clearly show an effect of hydrogen on the measured RA.

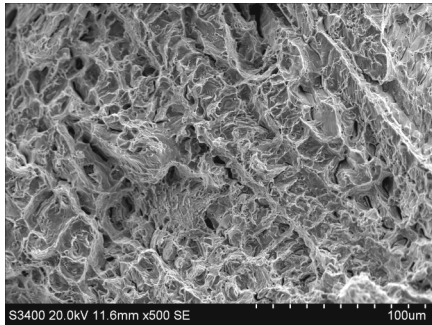


(a)

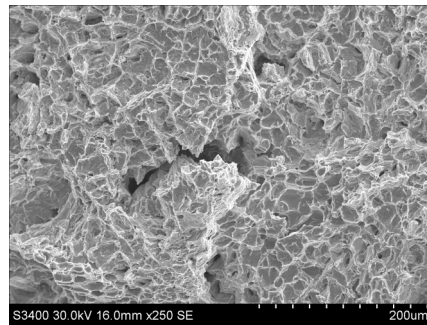


(b)

*Figure 2: Fracture features of welded smooth tensile specimens that appear to be associated with the solidified microstructure; (a) non-charged; (b) hydrogen-precharged.*



(a)



(b)

*Figure 3: Fracture surfaces of hydrogen-precharged welds; (a) smooth tensile specimen; (b) notched tensile specimen.*

Previous studies on austenitic stainless steel welds have shown that the ferrite in the weld plays an important role in hydrogen-assisted fracture [13, 14]. Interpretation of the fractographic evidence, however, is complicated by the inhomogeneity of the weld microstructures (Figure 1), which is reflected in a range of fracture features (Figures 2 and 3). The austenite-ferrite boundaries, nevertheless, appear to be an important attribute for hydrogen-assisted fracture in welded materials. The furrows that are observed on the fracture surfaces of the smooth tensile specimens, for example, are significantly sharper in the hydrogen-precharged condition (Figure 2b) compared to the non-charged condition (Figure 2a). This observation implies that hydrogen enhances fracture associated with the two-phase microstructure, in particular with the austenite-ferrite boundaries. Since cross is inhibited by hydrogen [16], the effectiveness of boundaries as obstacles to dislocation motion is enhanced, facilitating the pile-up of dislocations and contributing to the development of stress concentration at boundaries [14]. Local stress concentration at the austenite-ferrite boundaries can cause failure along these boundaries [14], or can induce cleavage fracture in the ferritic phase as observed for duplex stainless [12] and welds [13]. In either case, hydrogen-enhanced localized plasticity [16] is an important element for inducing fracture associated with these boundaries.

## SUMMARY

The effect of internal hydrogen was evaluated on the tensile properties of welded AISI 316 stainless steel. Although internal hydrogen significantly reduces RA, fracture is associated with plastic deformation in both annealed and welded microstructures. As compared to wrought annealed material, welded metal was found to be more susceptible to hydrogen-assisted fracture. Other studies have attributed hydrogen-assisted fracture in two-phase microstructures to hydrogen-enhanced stress concentration at austenite-ferrite boundaries. The results and observations of fracture surfaces in this study are consistent with this interpretation. Notches increase stress in the specimens, which contributes to further reduction of tensile ductility compared to smooth tensile specimens. Notches are particularly effective at reducing tensile ductility in two-phase microstructures (welds) exposed to hydrogen, since local stress concentrations at the boundaries due to hydrogen are further enhanced by the higher far-field stresses.

## REFERENCES

1. RJ Walter and WT Chandler. Effects of High-Pressure Hydrogen on Metals at Ambient Temperature: Final Report. Rocketdyne (report no. R-7780-1) for the National Aeronautics and Space Administration, Canoga Park CA (February 1969).
2. AW Thompson. Ductility Losses in Austenitic Stainless Steels Caused by Hydrogen. in: IM Bernstein and AW Thompson, editors. Hydrogen in Metals. Proceedings of the International Conference on the Effects of Hydrogen on Materials Properties and Selection and Structural Design (Champion PA, 1973), volume Metals Park OH: American Society of Metals (1974) p. 91-105.

3. GR Caskey. Hydrogen Compatibility Handbook for Stainless Steels (DP-1643). EI du Pont Nemours, Savannah River Laboratory, Aiken SC (June 1983).
4. JA Harris and MCV Wanderham. Propeties of Materials in High Pressure Hydrogen at Cryogenic, Room, and Elevated Temperatures. Pratt and Whitney Aircraft (report no. FR-5768) for the National Aeronautics and Space Administration (Marshall Space Flight Center), West Palm Beach FL (Jul 1973).
5. MR Louthan, GR Caskey, JA Donovan and DE Rawl. Hydrogen Embrittlement of Metals. Mater Sci Eng 10 (1972) 357-368.
6. C San Marchi, DK Balch, K Nibur and BP Somerday. Effect of high-pressure hydrogen gas on fracture of austenitic steels. J Pressure Vessel Technol 130 (2008) 041401.
7. C San Marchi and BP Somerday. Technical Reference on Hydrogen Compatibility of Materials (SAND2008-1163). Sandia National Laboratories, Livermore CA (2008).
8. C San Marchi, BP Somerday, X Tang and GH Schiroky. Effects of alloy composition and strain hardening on tensile fracture of hydrogen-precharged type 316 stainless steels. Int J Hydrogen Energy 33 (2007) 889-904.
9. C San Marchi, BP Somerday, X Tang and GH Schiroky. Hydrogen-assisted fracture of type 316 stainless steel at subambient temperature (PVP2008-61240). in: Proceedings of PVP-2008: ASME Pressure Vessels and Piping Division Conference, 2008, Chicago IL. ASME
10. L Zhang, M Wen, M Imade, S Fukuyama and K Yokogawa. Effect of nickel equivalent on hydrogen gas embrittlement of austenitic stainless steels based on type 316 at low temperatures. Acta Mater 56 (2008) 3414-3421.
11. C San Marchi, BP Somerday and SL Robinson. Permeability, Solubility and Diffusivity of Hydrogen Isotopes in Stainless Steels at High Gas Pressure. Int J Hydrogen Energy 32 (2007) 100-116.
12. C San Marchi, BP Somerday, J Zelinski, X Tang and GH Schiroky. Mechanical properties of super duplex stainless steel 2507 after gas phase thermal precharging with hydrogen. Metall Mater Trans 38A (2007) 2763-2775.
13. BP Somerday, DK Balch, M Dadfarnia, KA Nibur, CH Cadden and P Sofronis. Hydrogen-assisted crack propagation in austenitic stainless steel fusion welds. Metall Mater Trans (submitted) (2008).
14. JA Brooks and AJ West. Hydrogen Induced Ductility Losses in Austenitic Stainless Steel Welds. Metall Trans 12A (1981) 213-223.
15. JA Brooks and AW Thompson. Microstructural development and solidification cracking susceptibility of austenitic stainless steel welds. International Materials Review 36 (1991) 16-44.
16. HK Birnbaum and P Sofronis. Hydrogen-enhanced localized plasticity—a mechanism for hydrogen-related fracture. Mater Sci Eng A176 (1994) 191-202.